

# ANALYSIS OF CONDITIONS FOR OBTAINING A KEYHOLE REGIME FOR LASER WELDING

Remus Boboescu<sup>1</sup>

<sup>1</sup>University Politehnica Timișoara, [remus\\_boboescu@yahoo.com](mailto:remus_boboescu@yahoo.com)

**Abstract:** For laser welding using high intensity of laser beam produce the keyhole phenomenon in welding pool. For keyhole welding regime there is a particular of the weld cross-section shape aspect given by the heat affected zone area. It analyzes the laser welds made with Nd: YAG laser on low alloy steel plates using irradiation in continuously regime. The power, welding speed and defocusing are varied. Experiments were conducted after the full factorial experimental design 2<sup>2</sup>. This showed the effect of laser power for setting keyhole welding regime.

**Keywords:** *laser keyhole welding, full factorial design, laser beam defocusing, heat affected zone.*

## 1. Introduction

Laser welding has two distinct regimes of conduction welding and keyhole welding regime which differ in the weld penetration and weld cross section shape.

**Conduction welding regime.** This regime is called conduction limited welding. The solid-liquid interface heat transfer mechanism is exclusively by conduction. Heat is conducted directly from the heat source that occurs due laser radiation from the workpiece surface within the material. Conduction welding regime is characterized by irradiation sufficient to produce piece surface melting and vaporization but not enough to produce vaporization in the depth of material. For conduction welding regime values of F ratio between the weld width and weld depth are higher than 1,  $F \geq 1$ . As an indicative value for the weld depth in conduction regime is 1.5 mm [1]. Defects that are obtained in conduction welding regime are cracks on the weld surface.

**Keyhole welding regime.** This welding regime involves the keyhole phenomenon in weld pool which involves the values of laser beam intensities that exceed threshold needed to produce a vapor front propagation in the material. Heat transfer mechanism at solid-liquid interface involves both conduction and convection due to the melt movement in the weld pool. In weld cross section there is a welding defects gas bubbles, the presence of this pore led to the designation of keyhole regime (“key hole”). F ratio between weld width and weld depth has a smaller value than 1,  $F \leq 1$ .

Defects in welds are obtained for the keyhole welding regime are gas porosity due to dissolution into the melt a gas bubbles and vacuum large areas. The presence of the Keyhole and vapor within the material made pushing melting front (solid-liquid interface) inside the material. This provides increased weld penetration [2], [3], [4]. For welds made in experiments the two welding regimes are shown in Figure 1 by the weld cross section.

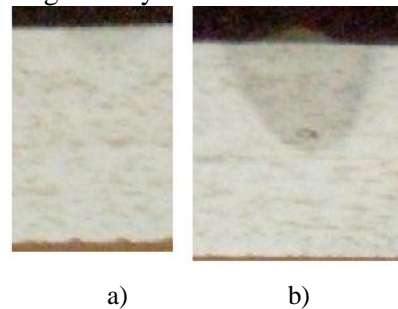


**Figure 1:** Image of weld cross-section of the weld a) weld in the conduction regime b) weld in keyhole regime

The paper proposes the identification and use of quantities that can characterize welds under keyhole welding regime. It looks like those in characterizing keyhole regime occurs sizes associated with both weld cross section and weld surface. Experimental factorial design 2<sup>2</sup> used presents for higher levels of power keyhole welding regime and for the lower power level presents the conduction welding regime. It will discuss variation of the response functions relative to varied parameters power and welding speed.

## 2. Experiments

The experiment consisted in made lines of fusion (welds), 110 mm long, on Dillimax 500 steel plates with thickness of 10 mm (carbon steel, carbon content  $\leq 0.16\%$ ). Was used a Nd: YAG Triumph Haas 3006D laser source with 3kW maximum power on a continuous wave regime CW. Laser beam was transmitted through a optical fiber with core diameter of 0.6 mm

The focus system made a focal spot with 0.6 mm diameter. Lens focal length was 200 mm. As protective gas argon was used with a flow rate of 20 l / min. Were used sheets of material with dimensions of  $100 \times 130 \times 10$  mm for which were made between 5 and 8 welds, with a distance of over 10 mm between welds. Parameters varied in the experiments are presented in Figure 2.

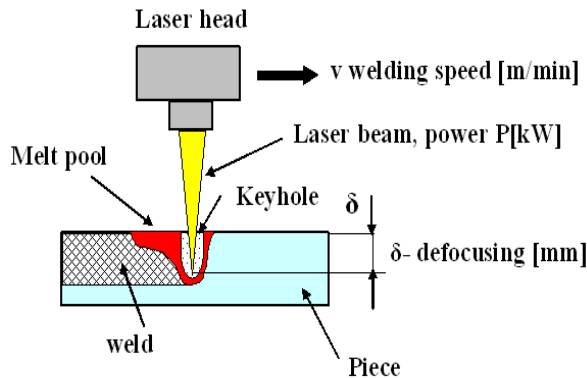


**Figure 2:** Scheme of keyhole welding pool with varied parameters in welding process

In experiments was varied the laser power, welding speed and distance between focal plane and piece surface (defocusing or defocusing depth) figure 2. Welds were cut in the stable part of the weld near the place where welding process was stopped. Weld section was processed metallographic. Weld width, near the piece surface, and weld depth were examined using a microscope with precision of 0.01 mm. Melted area was measured directly by its footprint.. Defocusing values are considered negative if the laser beam focus inside the piece.

In the experiments were varied power and welding speed. To statistically analyze the effects of parameters was necessary to introduce a dimensionless parameter values. Transformations between the two systems of parameters values (actual values and coded values) are based by following relationships:

$$A = P - 2 \quad (1)$$

$$B = -2.33 + 2.22v \quad (2)$$

The experimental plan is presented in Table 1 with actual values that coded for power and cutting speed.

**Table 1:** Varied parameters values in experiment

weld	power		speed	
	A [-]	P [kW]	B [-]	v [m/min]
1	-1	1	-1	0.6
2	+1	3	-1	0.6
3	-1	1	+1	1.5
4	+1	3	+1	1.5
5	0	2	0	1
6	0	2	0	1

Analysis procedure consisted of presenting the results of the mathematical model, ANOVA table showing the correlation coefficients associated with the mathematical model, Pareto chart showing the hierarchy of effects and response surface is a graphic representation of mathematical model. For the mathematical model were presented two forms for real values laser power and welding speed and for coded system values. The first allows rapid application of formulas and the second allows direct analysis of the values of regression coefficients. Based on these values were achieved Pareto charts. Figure 3 shows the analysis weld scheme and analyzed sizes that characterizing the weld.

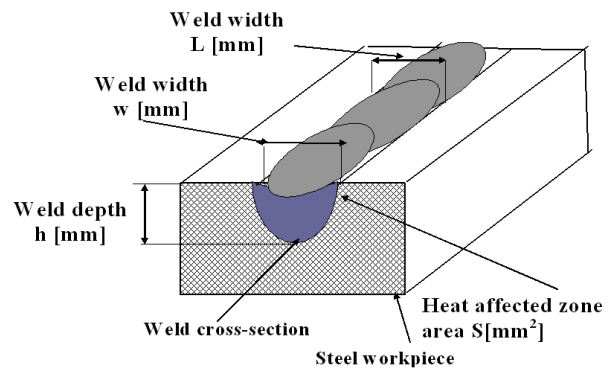


**Figure 3:** Scheme of weld with measured sizes

The paper analyzed variations the following sizes: weld width, shape ratio of weld cross section and the heat affected zone area on the weld cross section.

Weld width L [mm] was obtained as a result of three measurements on the weld surface at the beginning, middle and end of the welding process. The weld width characterized in general

the weld and it is independent of the area in this cross section in weld was performed.

F ratio (w/h) is the ratio between weld width and weld depth on the weld cross section.

This ratio is associated with the welding regime characterization. Values of F ratio below unity shows keyhole welding regime.

A heat affected zone area  $S[\text{mm}^2]$  was measured on the weld cross section. It is given by the isothermal line of transformation metal structure which is well below the melting temperature. Area heat affected zone containing molten zone area. Heat affected area can be measured with greater accuracy than the area of molten zone.

### 3. Weld width

The mathematical model for weld width at defocusing  $\delta = 0$  is given by relations (3) and (4). Statistical analysis by ANOVA method is given in Table 2. Figure 4 shows the Pareto chart for weld width at defocusing  $\delta = 0$ . It is noted that the weld width increases with power and decreases with welding speed.

The decrease effect with welding speed is greater than the increase effect of power. The interaction between power and welding speed increases width of the weld width so the overall effect of increasing with power exceeds the decreasing effect with welding speed. The Pareto diagram presented three effects have similar values and have no statistical significance. It looks like that along the weld there is a change for the first effect between power and welding speed.

$$L = 2.086 + 0.29A - 0.375B + 0.275 AB \quad (3)$$

$$L = -0.64859 + 0.93075P - 2.0535v + 0.61050Pv \quad (4)$$

**Table 2:** ANOVA table for weld width  $L$  at  $\delta = 0$

Effect	Sum of Squares	DF	Mean Sq.	f-Ratio	P-val
A(power)	0.336	1	0.336	2.6	1.1
B(speed)	0.562	1	0.562	4.24	0.22
AB	0.302	1	0.302	2.34	0.26
Total error	0.258	2	0.129		
Total (corr)	1.460	5			
$R^2 = 0.82$		$R^2(\text{adj. for d.f.}) = 0.55$			

**Pareto Chart for weld width  $L$ ,  $\delta = 0$**

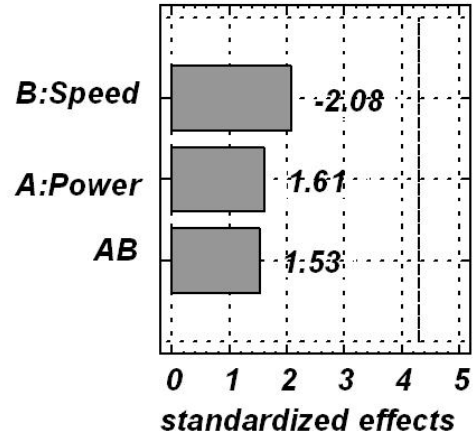


**Figure 4:** Pareto Chart for weld width at  $\delta = 0$

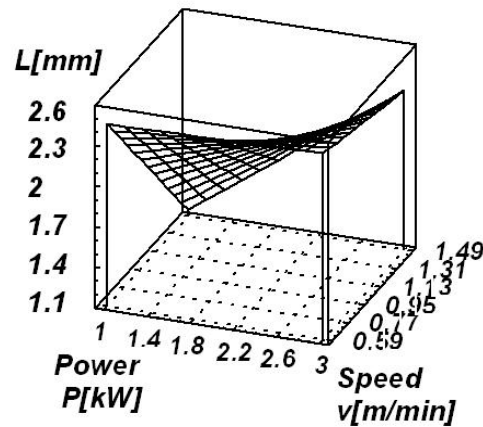


**Figure 5:** Response surface for weld width at  $\delta = 0$

Figure 5 shows the surface response for weld width at defocusing  $\delta = 0$ . It is noted that the weld width has high values on the experimental field. Lower values for the weld width are obtained at low power and high welding speeds. There is a sharp increase in weld width values on the diagonal of experimental field from low power and high welding speed on the situation in which power is high and low welding speed. It is recommended for high value of weld width. These values can be associated with deep welds.

The mathematical model for weld width at defocusing  $\delta = -2\text{mm}$  is given by equations (5) and (6). The correlation coefficients for the mathematical model associated with the mathematical and statistical method of ANOVA analysis of variances are given by equations (7) and (8).

Figure 6 shows the Pareto diagram for the weld width at defocusing. It is noted that the weld width increases with power and decreases with welding speed. Effect of power have statistical significance. The interaction between power and welding speed decreases weld width. It is noted that the cumulative effect of decreasing of the weld width with welding speed is lower than the increase with power. This shows the strong dependence of the weld width with power.

$$L = 2.0966 + 0.875 A - 0.545 B \quad (5)$$

$$- 0.325 AB$$

$$L = 0.10195 + 1.63225 P + 0.23310 v \quad (6)$$

$$- 0.72150 P v$$

$$R^2 = 0.95 \quad (7)$$

$$R^2(\text{adj. for d.f.}) = 0.87 \quad (8)$$

**Pareto Chart for weld width L,  $\delta = -2mm$**

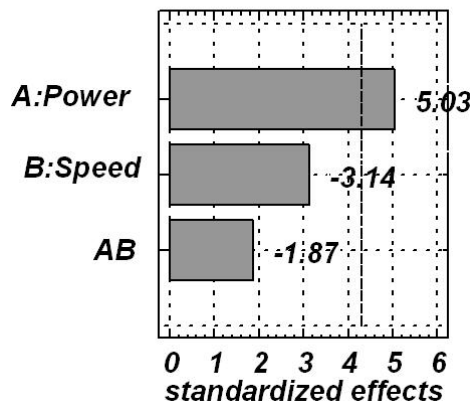


**Figure 6:** Pareto Chart for weld width at  $\delta = -2mm$

Figure 7 shows the response surface for the weld width at defocusing  $\delta = -2mm$ . It is noted that on the experimental field weld width increases with power and decreases with welding speed. Maximum values for weld width are obtained for the maximum power and minimum welding speed. The type of increase seen in Figure 5 exists in this case for focusing within piece. The difference that arises is that this type of growth is valid throughout the experimental field.

Focusing the laser beam inside the piece brings the following changes relative to the weld width. By focusing a laser beam inside the piece produce a control of weld width through its dependence on power and association of this dependence to statistical significance. Focus inside piece changes sign of interaction between power and speed.

To focus on the piece surface effect of the interaction is associated with speed effect, for focus within the piece the interaction effect is associated with power effect. This shows the increased contribution of dynamic phenomena that occurring in the weld pool. It shows that the laser beam focus inside the piece provides stability on weld width and for overall the weld surface characteristics of welds.

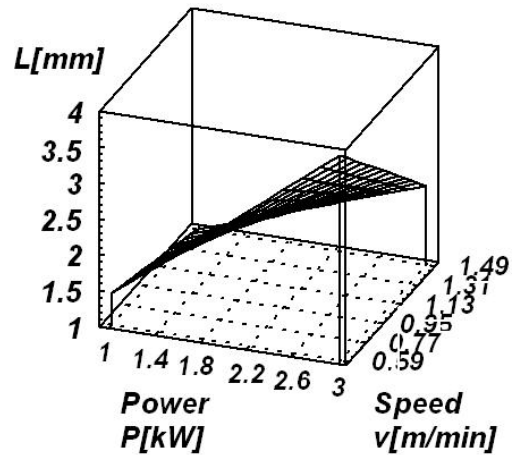


**Figure 7:** Response surface for weld width at  $\delta = -2mm$

**4. Ratio F**

The mathematical model for the ratio F at defocusing  $\delta = 0$  is given by equations (9) and (10). Study of variation by the ANOVA method is presented in Table 3.

$$F = 1.535 - 1.025A - 0.375B - 0.425 AB \quad (3)$$

$$F = 6.43925 - 2.01525P + 2.7195v - 0.9435Pv \quad (4)$$

**Table 3:** ANOVA table for Ratio F at  $\delta = 0$

Effect	Sum of Squares	DF	Mean Sq.	f-Ratio	P-val
A (power)	4.202	1	4.202	11.85	0.07
B (speed)	0.562	1	0.562	1.59	0.33
AB	0.722	1	0.722	2.04	0.28
Total error	0.709	2	0.354		
Total (corr.)	6.196	5			
$R^2 = 0.88$		$R^2(\text{adj. for d.f.}) = 0.71$			

Figure 8 shows the Pareto chart for the ratio F at defocusing  $\delta = 0$ . Decreased of ratio F shows getting keyhole welding regime and increase its intensity. The figure notes that the experimental field F Ratio strongly decreases with power. Effect of interaction between power and welding speed

decreases the ratio F. Welding speed increases Ratio F. The overall effect of power is much higher than the welding speed effect. The three effects have not shown statistically significance.

$$F = 1.71 - 1.0925 A - 0.2425 B + 0.2275 AB \quad (11)$$

$$F = 5.520175 - 1.622575 P - 1.548450 v + 0.505050 Pv \quad (12)$$

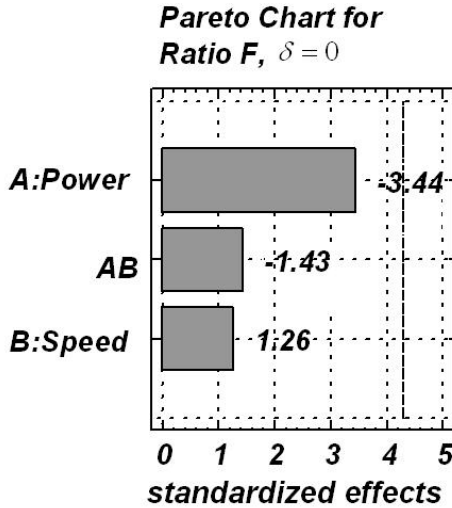


Figure 8: Pareto Chart for ratio F at  $\delta = 0$

Response surface shown in Figure 9 indicates that the F ratio decreases with the power and welding speed on the experimental field. Lowest values for the F ratio are obtained at high power and low welding speeds. At high power welding speed has no influence. In this situation gets keyhole welding regime. Conduction welding regime is carried out at low power and high speed welding.

It notes that there is a sudden transition from conduction welding regime to the regime keyhole welding.

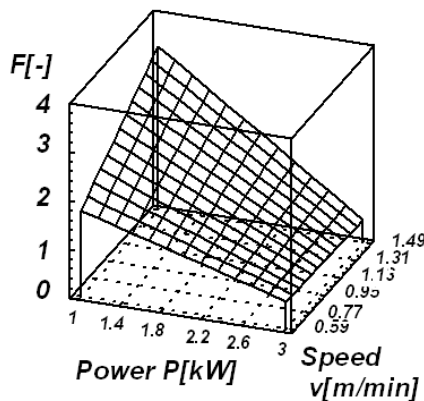


Figure 9: Response surface for Ratio F at  $\delta = 0$

The mathematical model for the ratio F at defocusing  $\delta = -2mm$  is given by equations (11) and (12). Study the variations by ANOVA method is presented in Table 4.

Table4:ANOVA table for Ratio F (w/h)at  $\delta = -2mm$

Effect	Sum of Squares	DF	Mean Sq.	f-Ratio	P-val
A(power)	4.774	1	4.774	7.32	0.11
B( speed)	0.235	1	0.235	0.36	0.61
AB	0.207	1	0.207	0.32	0.63
Total error.	1.305	2	0.652		
Total (corr.)	6.521	5			

$R^2 = 0.79$        $R^2$  (adj. for d. f.) = 0.49

Figure 10 shows the Pareto chart for the ratio F at defocusing  $\delta = -2mm$ . It is noticed that the experimental field F ratio decreases with power and also decreases with welding speed. The only effect that increases the ratio F is given by the interaction between power and welding speed. The effects have not shown statistically significance. It is shown that both increased with power and welding speed leads to increased intensity of keyhole welding regime. Focusing the radiation inside the piece provides propagation and absorption of radiation in Keyhole. High welding speed leads to the production of two spots in which the laser radiation absorption takes place. So this may lead to loss of the radiation out of keyhole by reflection, situation shown by the interaction between power and welding speed.

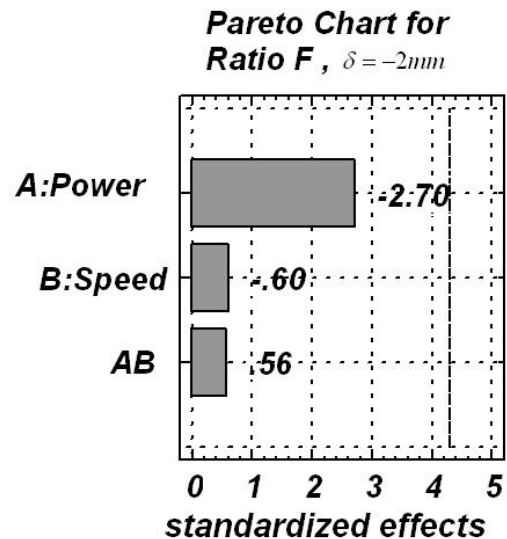


Figure 10: Pareto Chart for Ratio F at  $\delta = -2mm$

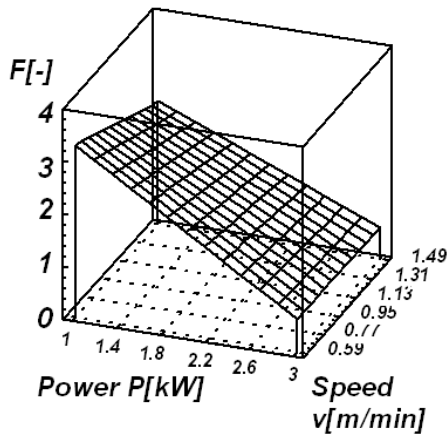


Figure 11: Response surface for Ratio  $F$  at  $\delta = -2\text{mm}$

Response surface in Figure 11 shows the variation ratio  $F$  at defocusing  $\delta = -2\text{mm}$ . It is noticed that on experimental field the  $F$  ratio decreases with power. Welding speed do not produce significant changes. It looks as if the laser beam focus within the piece setting of keyhole welding regime depends solely on power.

Focusing the laser beam inside the piece, compared with focusing on the piece surface, increased the role of power in the setting of the keyhole welding regime. It notes the changing role of the interaction effect between power effect and welding speed effect.

### 5. Heat affected zone area on the weld cross section

The mathematical model for heat affected zone area on weld cross section at defocusing is given by equations (13) and (14). ANOVA statistical analysis method is presented in Table 5.

$$S = 9.25 + 6.875 A - 3.875 B - 3.125 AB \quad (13)$$

$$S = 1.03375 - 0.40625 P + 5.2725 v - 6.9375 Pv \quad (14)$$

Table 5: ANOVA table for HAZ area  $S$  at  $\delta = 0$

Effect	Sum of Squares	DF	Mean Sq.	f-Ratio	P-val
A(power)	189.62	1	189.62	39.03	0.2
B(speed)	60.062	1	60.062	12.40	0.7
AB	39.062	1	39.062	8.06	0.1
Total error	9.68	2	4.843		
Total (corr.)	297.875	5			
$R^2 = 0.96$		$R^2$ (adj. for d. f) = 0.91			

Pareto Chart for Heat affected zone area  $S$ ,  $\delta = 0$

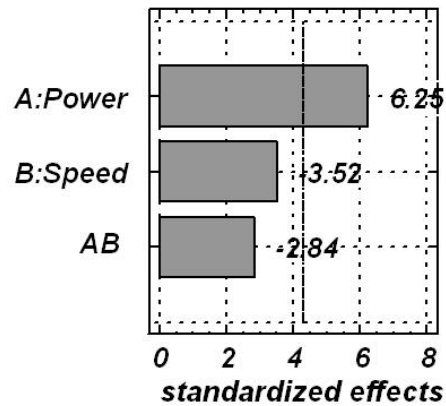


Figure 12: Pareto Chart for HAZ area at  $\delta = 0$

Figure 12 shows the Pareto chart for the area of heat affected zone to focus on the piece surface.  $\delta = 0$ . It is noted that the area of heat affected zone increases with power and decreases with welding speed. Power effect is statistically significant. The interaction between power and welding speed decreases the area of heat affected zone. The overall decrease effect with welding speed is stronger than the increase effect with power. It is noted that all three effects are important contributions for determining the heat affected zone area.

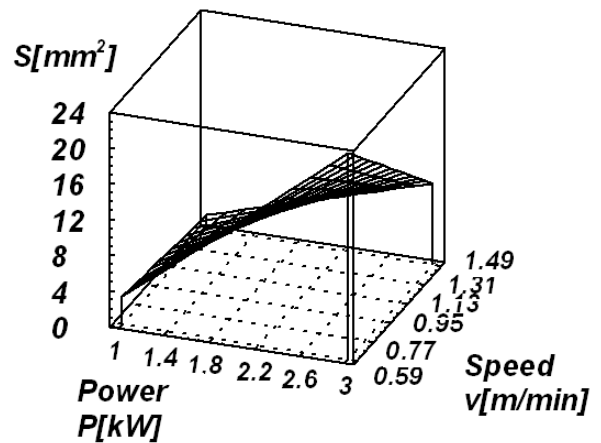


Figure 13: Response surface for HAZ area at  $\delta = 0$

Figure 13 shows the response surface for area of the heat affected zone at defocusing  $\delta = 0$ . It is noted that on the experimental area of heat affected zone increases with power and decreases with welding speed on the field experiment. The highest values for the area is obtained at high power and low welding speed.

The mathematical model for heat affected zone area on the weld cross section at defocusing  $\delta = -2mm$  is given by equations (15) and (16). ANOVA statistical analysis method is presented in Table 6.

$$S = 9.4166 + 8.125 A - 3.875 B - 2.625 AB \quad (15)$$

$$S = -10.03715 + 14.24125 P + 3.05250 v - 5.82750 P v \quad (16)$$

**Table 6:** ANOVA table for HAZ area  $S$  at  $\delta = -2mm$

Effect	Sum of Squares	DF	Mean. Sq.	F-Ratio	P-val
A(power)	264.062	1	264.062	45.84	0.02
B(speed)	60.062	1	60.062	10.43	0.08
AB	27.562	1	27.562	4.78	0.16
Total error	11.520	2	5.76		
Total (corr.)	363.208	5			
$R^2 = 0.96$		$R^2$ (adj. for d.f.) = 0.92			

**Pareto Chart for Heat affected zone area  $S$ ,  $\delta = -2mm$**

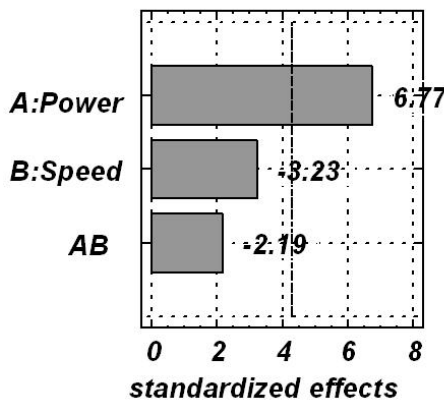


**Figure 14:** Pareto Chart for HAZ area at  $\delta = -2mm$

Figure 14 presents the Pareto chart for the area of heat affected zone at defocusing  $\delta = -2mm$ . It is noted that the area of heat affected zone increases with power and decreases with welding speed. The interaction between power and welding speed decreases the area of heat affected zone. Power is the only effect that has statistical significance.

Response surface in Figure 15 shows the variation in heat affected zone area on weld cross section at defocusing  $\delta = -2mm$ . It is noted that in the experimental field heat affected zone area increases with power and decreases with welding speed. Variations with welding speed are strongest at high power than at low power.

Response surface deformation on experimental field is due by the interaction between power and welding speed effect.

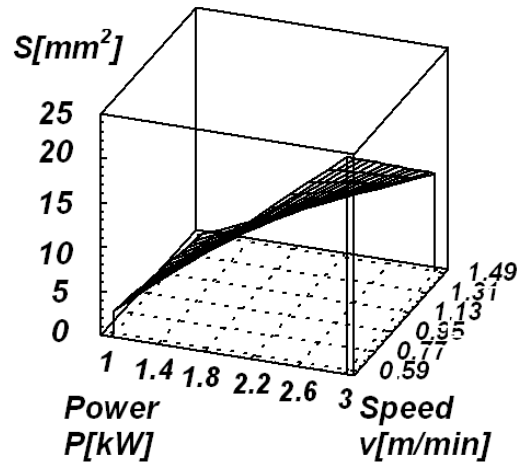


**Figure 15:** Response surface for HAZ area at  $\delta = -2mm$

For heat affected zone area laser beam focus within the piece led to an increase in the role of power. This increase is relatively small. At focus within the piece the effect of the interaction between power and welding speed decreases.

**6. Discussion**

Laser welding is widely applied in particular for metals and steel. The laser beam is a concentrated heat source.

In laser welding Keyhole phenomenon has two important consequences. The first relates to increasing the energy coupling between laser radiation and material because the laser radiation can propagate in the Keyhole and its absorption occurs inside the material. This creates the possibility of formation of heat sources inside the material. It is considered that the presence of Keyhole will increase the energy coupling between laser radiation and material.

The second issue concerns the very strong growth of Keyhole in the depth of material. The presence of a strong heat source that produces sudden changes in time and space heating favors strong evaporation. Vaporization is followed by a rapid increase in pressure followed by high in vaporization temperature. Such gas-liquid interface becomes overheated. Rapid disappearance of the irradiated heat source will produce rapid vaporization of superheated liquid by passing the vapor.

In this paper we studied the variation of the three sizes that characterize welds in keyhole

welding regime for two situations for the depth of focus. Keyhole welding regime was obtained for high values of power. The Ratio F shows subunit values for keyhole welding regime. These F ratio values are associated with high values of weld width and with high values heat-affected zone area on the weld cross section.

It looks like that all the three sizes analyzed in the paper, weld width, Ratio F, heat affected zone area can be used to separate the welds in the conduction regime by the welds in keyhole regime. Although the F ratio criterion defines the separation between the two welding regimes, the mathematical models for the weld width and area of heat affected zone are useful in predicting welding regime obtained. Focusing on the surface of the piece introduces instabilities in the welds. These are associated with the lack of statistical significance for the mathematical models associated with one dimensional size for welds. Weld instabilities produced by focus on piece surface are more pronounced for weld width, size that characterizes the weld surface. Heat affected zone area shows small with defocusing. Mathematical models have shown high levels of correlation coefficients.

## 7. Conclusions

The paper presents two important issues for the study of welds made with laser beam the presence of keyhole regime and the effect of defocus for laser beam. For analysis of the welding process was used a full factorial experimental design and were used mathematical modeling and statistical analysis of variations. The following were showed:

- The weld width and heat affected zone area on the weld cross section can be used to characterize the welding regime as well as the F ratio.
- For high power levels were obtained welds in keyhole welding regime.
- Focusing the laser beam to the workpiece surface produces instability in the welding process.
- Defocusing change did not affect the welding regime obtained as evidenced by effects on the heat affected zone area.

The aim of experimental study was the assessing contribution of power and speed of welding to weld characteristics. From the analysis carried out were the following: power has main effect on all response function and in conclusion for laser melt capacity; power increase laser melting capacity of steel and welding speed decrease this capacity; mathematical models for

the weld width and weld depth provided a good statistical correlation and statistical significance. The experimental modeling achieved considered only the main part of the laser processing. There have been lines fusion lines and not welded joints. Were varied only main factors of influence, power and speed, while focal point position in relation with the piece surface and assistant gas parameters was maintaining constant. The plates used were sufficient thick to not be penetrated during welding. It is important that experimental research should be applicable in slightly modified experimental conditions. To fill the gap between tow pieces using at laser welding using added material in the form of wire. Mathematical models performed make predictions for the laser welding results for Dillimax 500 steel or other steels with close thermal characteristics. Experimental research methods used are generally applicable in material processing.

## References

- [1] Alexander F. H. Kaplan, Masami Mizutani, Seiji Katayama, Akira Matsunawa, *Keyhole Laser Spot Welding*, International Conference Applications of Lasers and Electro-Optics 2002
- [2] Yukimichi Sasaki , Tadashi Misu , Shunro Yoshioka , and Toshiyuki Miyazaki, *Monitoring of YAG Laser Spot Welding-Detection of Porosity Defect by Acoustic Signal* International Conference Applications of Lasers and Electro-Optics 2002.
- [3] Inoue, Miamoto, Ono, Adachi, Matsumoto, *In process monitoring of penetration depth in 20 class CO<sub>2</sub> laser welding of thick sections*, International Conference Applications of Lasers and Electro-Optics 1999.
- [4] Jae Y. Lee, Sung H. K., Dave F. Farson, Choong D. Yoo, *Mechanism of keyhole formation and stability in stationary laser welding*, J. Phys. D: Appl. Phys. 35 (2002) 1570–1576.